TRIBHUVAN UNIVERSITY

INSTITUTE OF ENGINEERING

PULCHOWK CAMPUS

THESIS NO : M-86-MSMDE-2021-2024

MODAL ANALYSIS OF MULTI-DISK ROTOR SYSTEM

by

SUNIL PRADHAN

A THESIS

SUBMITTED TO THE DEPARTMENT OF MECHANICAL AND AEROSPACE ENGINEERING IN PARTIAL FULFILLMENT OF THE REQUIREMENTS FOR THE DEGREE OF MASTER OF SCIENCE IN MECHANICAL SYSTEMS DESIGN AND ENGINEERING

DEPARTMENT OF MECHANICAL AND AEROSPACE ENGINEERING

LALITPUR, NEPAL

JUNE 2024

COPYRIGHT

TRIBHUVAN UNIVERSITY

INSTITUTE OF ENGINEERING

PULCHOWK CAMPUS

DEPARTMENT OF MECHANICAL AND AEROSPACE ENGINEERING

The undersigned certify that they have read, and recommended to the Institute of Engineering for acceptance, a thesis titled **'MODAL ANALYSIS OF MULTI-DISK ROTOR SYSTEM'** submitted by **SUNIL PRADHAN (078/MSMDE/019)** in partial fulfillment of the requirements for the degree of Masters in Mechanical Systems Design and Engineering.

Prof. Dr. Mahesh Chandra Luintel
Supervisor
Department of Mechanical and Aerospace Engineering

Asst Professor Er. Janak Kumar Tharu
External Examiner
Department of Civil Engineering
Nepal Engineering College

Committee Chairperson, Asst Prof. Sudip Bhattrai
Head of the Department
Department of Mechanical and Aerospace Engineering

Tribhuvan University
Institute of Engineering
Department of Mechanical and Aerospace Engineering
Pulchowk Campus

Date: 2024/06/09

ABSTRACT

Controlling vibrations is essential for the safe and efficient operation of rotating machinery in industries such as aerospace, automotive, and power generation. This study focuses on the modal behavior of multi-disk rotor systems, a critical area in mechanical engineering. Employing a combination of analytical and mathematical modeling, alongside ANSYS-based simulations, this research investigates the modal characteristics and dynamic response of such systems. Key methodologies included the application of modal analysis in ANSYS to determine natural frequencies and mode shapes. The study specifically analyzed backward whirl and forward whirl frequencies. Results indicate that the first three natural frequencies for the system were found to be 67.155 Hz, 72.437 Hz, and 94.736 Hz for forward whirl under free response conditions. These values closely matched the theoretical predictions obtained from the mathematical model, with less than a 5% deviation.

Furthermore, the critical speeds identified for the system of first mode of transverse vibration was found to be 459.83 rad/s correlating with the key rotational velocities at which significant vibrations occur. This detailed analysis not only demonstrates the alignment between computational and analytical methods but also highlights the critical frequencies that necessitate attention in rotor system design to prevent operational failures and enhance performance.

ACKNOWLEDGEMENT

First and foremost, I want to thank my supervisor Asst. Prof. Mahesh Chandra Luintel, PhD, for his continuous support and guidance on this research.

I can never thank enough the duo: dear friend Er. Madhav and dear brother Sanjeev Karki for their unwavering technical assistance throughout the research. I am also grateful to Janak Tharu and Sandip Gewali for their insightful discussions regarding Vibrations and ANSYS.

Moreover, I am thankful to the Department of Mechanical and Aerospace Engineering for facilitating us with computational resources for solving the research problem.

I am also grateful towards the master's Program - MSMDE - Coordinator, Prof. Dr. Laxman Poudel for continuous guidance regarding various practical aspects of life.

I, furthermore, would like to convey my special thanks to Asst. Prof. Mahesh Chandra Luintel, Ph.D., for introducing me to the beautiful field of multi-rotor system.

Also, many thanks to the classmates of MSMDE batch 2078 for a thoughtful environment throughout the master's study.

TABLE OF CONTENTS

LIST OF FIGURES

LIST OF TABLES

LIST OF SYMBOLS

Ω	Shaft Spin speed of, rad/s
ρ	Shaft Density, kg/m^3
ρ_1	Disk-1 Density, kg/m^3
ρ_2	Disk-2 Density, kg/m^3
A	Cross-sectional Area of Shaft, m^2
E	Modulus of Elasticity, Pa
i,j,k	Unit vectors along x, y, and z axes
I_s	Second moment of area of shaft section, m^4
I_1	Second moment of area of Disk 1 section, m^4
I_2	Second moment of area of Disk 2 section, m^4
J_{ps}	Polar second moment of area of shaft section, m^4
J_{p1}	Polar second moment of area of Disk 1 section, m^4
J_{p2}	Polar second moment of area of Disk 1 section, m^4
K_i	Modal Stiffness
L	Length of the shaft, m
M_1	Mass of Disk 1, kg
M_2	Mass of Disk 2, kg
r_s	Position vector of any point of shaft
T	Kinetic Energy
U_s	Strain Energy of the shaft
q_v	Displacement along y axis
q_w	Displacement along z axis
v_s	Velocity vector of any point of the shaft

CHAPTER ONE: INTRODUCTION

This chapter established the work conducted for this thesis and sheds light on the statement of problem and objectives.

1.1 Background

Rotating machinery is frequently employed in many different industries, including industrial, automotive, and aerospace. For these types of equipment to operate safely and effectively, the appropriate operation is essential. The rotor system's dynamic behavior is one of the key problems with rotating machinery. A shaft and one or more disks installed on the shaft make up a rotor system. In some circumstances, the mass of the rotor system may be out of balance, which can lead to vibrations and other dynamic issues.(Childs, 1993)

These systems are employed in turbines, compressors, and pumps in power production systems. Vibrations caused by the imbalanced mass may reduce the system's effectiveness and speed up deterioration(Chen et al., 2020). In addition, a variety of other industrial uses, including machinery for manufacturing, wind turbines, and marine propulsion systems, utilize rotor systems with several disks and an imbalanced mass. Controlling the vibrations is crucial for the system's safe and effective functioning in all these applications since the system's dynamic behavior is crucial(Chen et al., 2020).

Mechanical engineering dynamic analysis of rotor systems with multiple disks and an unbalanced mass is a crucial area of research. These systems have complex behavior, and vibrations can cause wear, fatigue, and other failures. Thus, it's essential to comprehend how these systems behave dynamically and create plans for reducing vibrations and enhancing performance.

Prior studies have used a variety of techniques, including experimental testing, analytical modeling, and finite element analysis, to examine the dynamic behavior of rotor systems with numerous disks and imbalanced masses (FEA) (Chiu, 2015). Some of this research concentrated on how the imbalanced mass affected the system's critical speed and natural frequency, while others looked at how the stiffness and mass distribution of the disk affected the system's behavior (Chiu, 2015).

The dynamic behavior of rotor systems with many disks and an uneven mass, however, still needs more research. This system behavior is greatly influenced by a number of variables, including the stiffness of the system, the position of the imbalanced mass, and the mass distribution of the disks. To comprehend the behavior of the system and create efficient strategies for enhancing its performance, a thorough examination of these elements is thus required.

In this thesis, it was suggested that analytical and mathematical modelling, followed by simulation using the ANSYS platform, be used to study the dynamic behavior of a rotor system with numerous disks and one unbalanced mass.

1.2 Problem Statement

Mechanical engineering research is heavily focused on the dynamic behavior of rotor systems with many disks and an imbalanced mass. These systems have complicated behavior, and vibrations can cause wear, fatigue, and other issues. For these systems to function safely and effectively, it is essential to have a thorough grasp of their dynamic behavior.

The issue with rotor systems with several disks and an imbalanced mass is that their dynamic behavior depends significantly on a number of variables, including the disks' mass distribution, where the unbalanced mass is located, and how stiff the system is. As a result, it is difficult to precisely forecast the system's behavior, and creating efficient ways to manage the vibrations and enhance their performance is a demanding challenge.

Also, earlier research has used a variety of techniques, including experimental testing, analytical modelling and FEA, to examine the dynamic behavior of rotor systems with numerous disks and imbalanced masses. The goal of this thesis is to use analytical and mathematical modelling to examine the modal behavior of a rotor system with two disks.

1.3 Objectives

Main Objective

The main objective of this thesis is to study the modal response of a multi-disk system (rotor-system).

Specific objective

- To develop a mathematical model for the vibration of a multi-disk system.
- To determine the analytical solutions of the free response of the system.
- To simulate the problem and compare the simulation results with analytical results.

1.4 Scope of the Work

The scope of this research work is limited to the modal analysis of a multi-rotor disk system. It focuses on determining the natural frequencies and mode shape of the system without considering any external forces such as jet forces or imbalanced masses. The considering layout consisting of two disks attached to the shaft with equal distance from the rigid bearings.

1.5 Assumptions:

Following assumptions are taken for the development and analysis of the mode:

- The disks are considered rigid.
- Shafts are considered flexible.
- Bearings are considered rigid.
- There is no longitudinal displacement of any point of the shaft.

CHAPTER TWO: LITERATURE REVIEW

2.1 Rotodynamic Fundamentals

Most of the rotating system is made up of a disc attached to a shaft and a shaft supported by bearings as shown in **Figure 2.1** and this combination can be taken as a rotodynamic system.

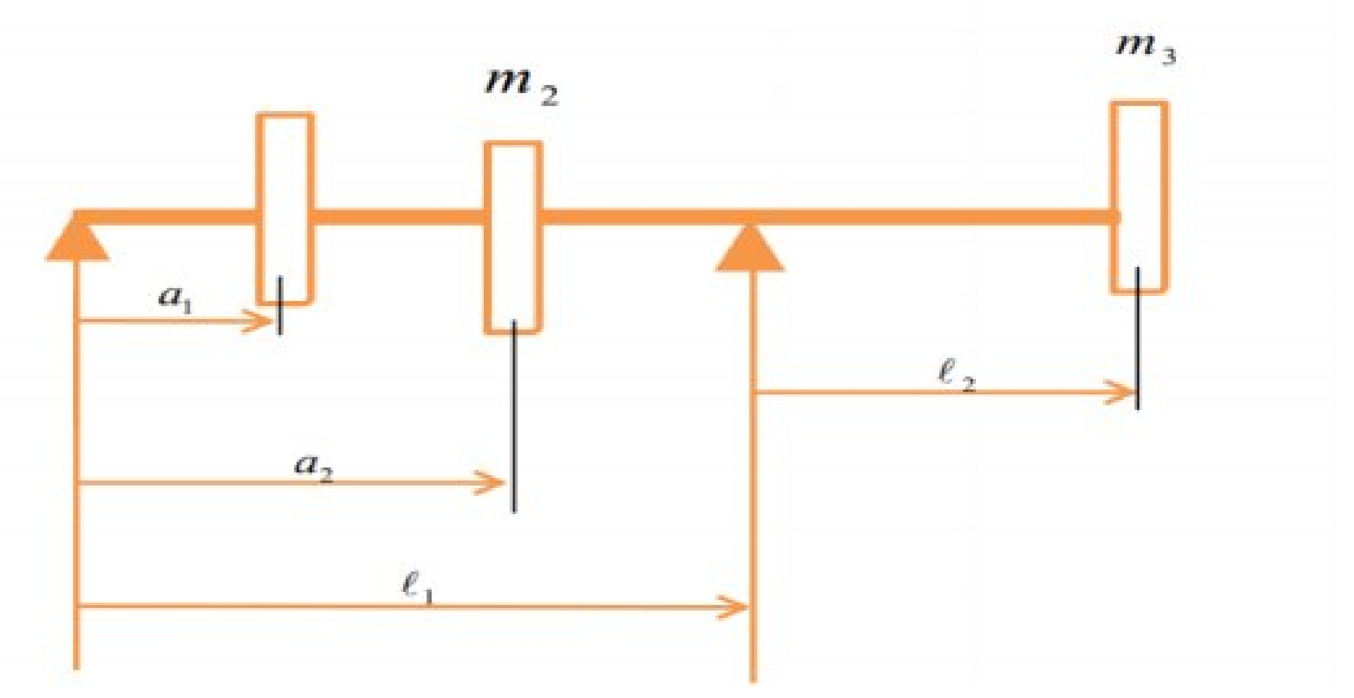

Figure 2.1*: Continuous Shaft and Disk Design(Kushwaha & Patel, 2023)*

The fundamental concepts and themes of Rotodynamic are presented(Ling, n.d.). A research model was developed before addressing certain physical characteristics of these types of structures. Based on this model, several typical Rotodynamic analysis options are investigated, the results of which are relevant for objectively describing the lateral dynamic behavior of rotors, thus providing a comprehensive understanding to the reader seeking a basic introduction to this topic. The consequences of a torsional moment acting on the shaft on its bending behavior will not be explored.

Depending on the application, each of the system's main components, namely the disc, shaft, and bearings, might be assumed to be rigid or flexible. Different combinations of these assumptions make up the many models of the same thing. The presence of an imbalance on the rotor is a typical source of rotor excitation. A straightforward method for incorporating the effect of this stimulation will be described(Luintel, n.d.-a).

If the shaft is assumed to be a massless flexible system, a discrete model can be used for the dynamic analysis; if the mass of the shaft cannot be ignored, a continuous model should be utilized. Any rotodynamic system's continuous shaft can be modelled as a rotating Euler-Bernoulli beam. In the Euler-Bernoulli beam theory, shear deformations are neglected, and plane sections remain plane and normal to the longitudinal axis.

Vibration analysis of the multi-disk rotor system can be conducted for longitudinal, transverse, torsional vibrations, or any combination of these modes. However, longitudinal vibration

analysis is relatively less common since it is not typically a critical concern that arises in most systems.

2.2 Common terminologies of Rotodynamic system

A dynamic analysis of a rotating system is performed to better understand its behavior and to investigate the influence of system characteristics and environmental interactions on its performance. The following section discusses common rotodynamic system terms.

2.2.1 Whirling

When the system rotates, the rotor experiences two fundamental lateral vibratory phenomena that function in tandem to determine the rotor's vibration modes: shaft bending and precessional whirling. When a shaft-disk system is placed in motion, it includes spin as well as movement of the shaft axis in a plane perpendicular to the bearing axis. Whirling refers to the movement of the shaft. As with any free vibration system, the frequency of whirl is determined by the stiffness and damping of the rotor(Luintel, n.d.-b). In the case of forced vibration, the whirl amplitude is a function of the frequency and amount of the excitation force(Kandouci et al., 2023).

When the motion of the deflected shaft is in the same direction as that of the spinning direction, it is called forward whirling and if it is in opposite direction of spin, it is called backward whirling.

Forward whirling and Back whirling are shown in **Figure 2.2.**

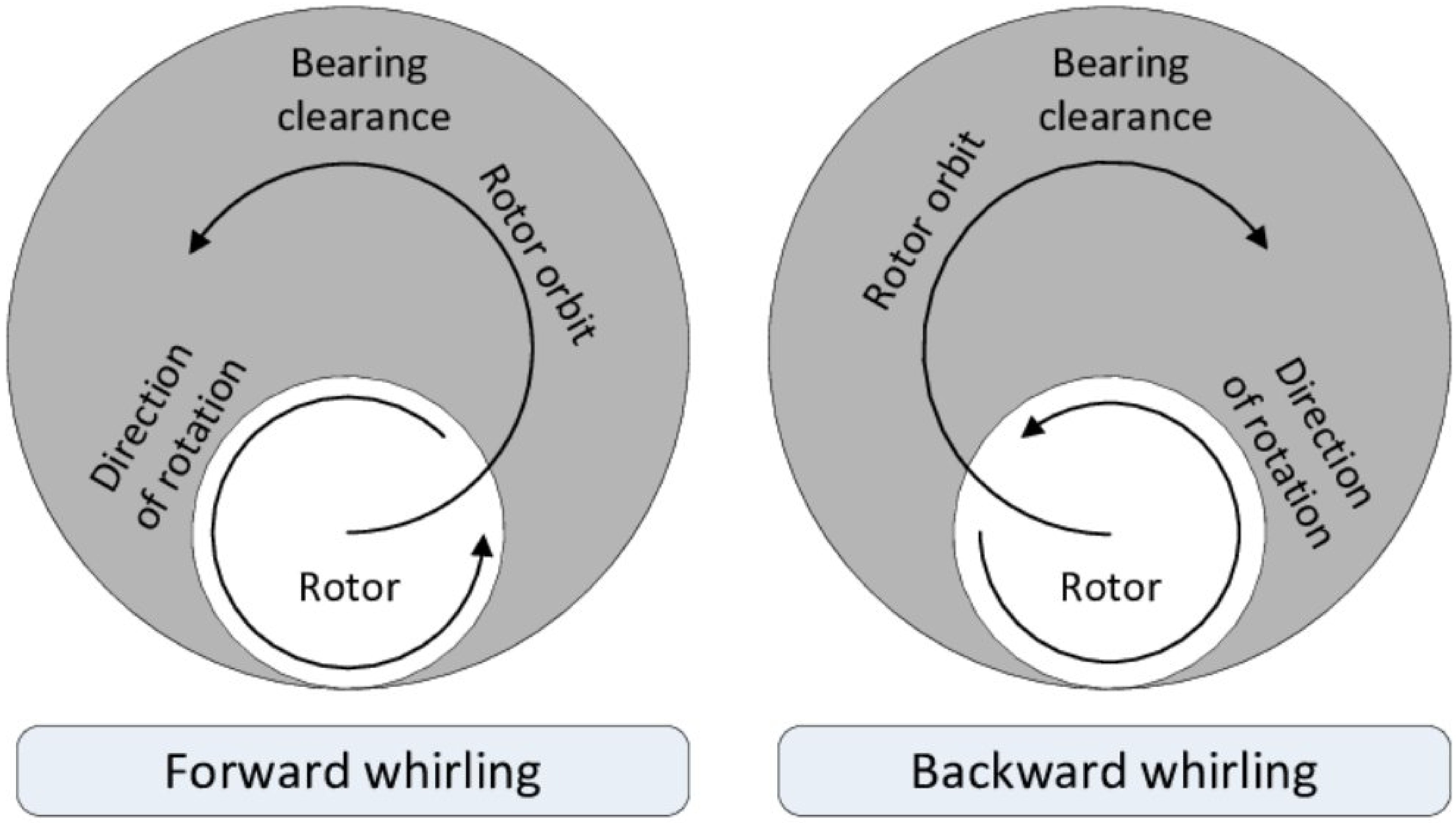

Figure 2.2: *Whirl Dynamics in Rotating Shaft-Disk Systems* (Delevitation Modelling of an Active Magnetic Bearing Supported Rotor, n.d.)

2.2.2 Critical Speed and Campbell Diagram

Critical speed, often referred to as "whirling speed" or "resonance speed", is the rotational velocity at which a machine's natural frequency coincides with the excitation frequency, leading to excessive vibrations and potential failure. This phenomenon is particularly relevant in applications involving shafts, axles, and rotating components. The critical speed of a beam or a shaft at rest is determined only by the system's mass/inertia and stiffness. The occurrence of critical speed can result in amplified vibrations, reduced operational lifespan, and even catastrophic breakdowns.

The Campbell diagram is a graphical representation of a rotating system's stability. It is used to show the dependency of the operating speed on the critical speed of the system. Each curve on the diagram corresponds to a mode of vibration, showing the regions of stability and potential instability as the rotational speed increases (Lu, Tao. (2019). A typical Campbell diagram is shown in **Figure 2.3**.

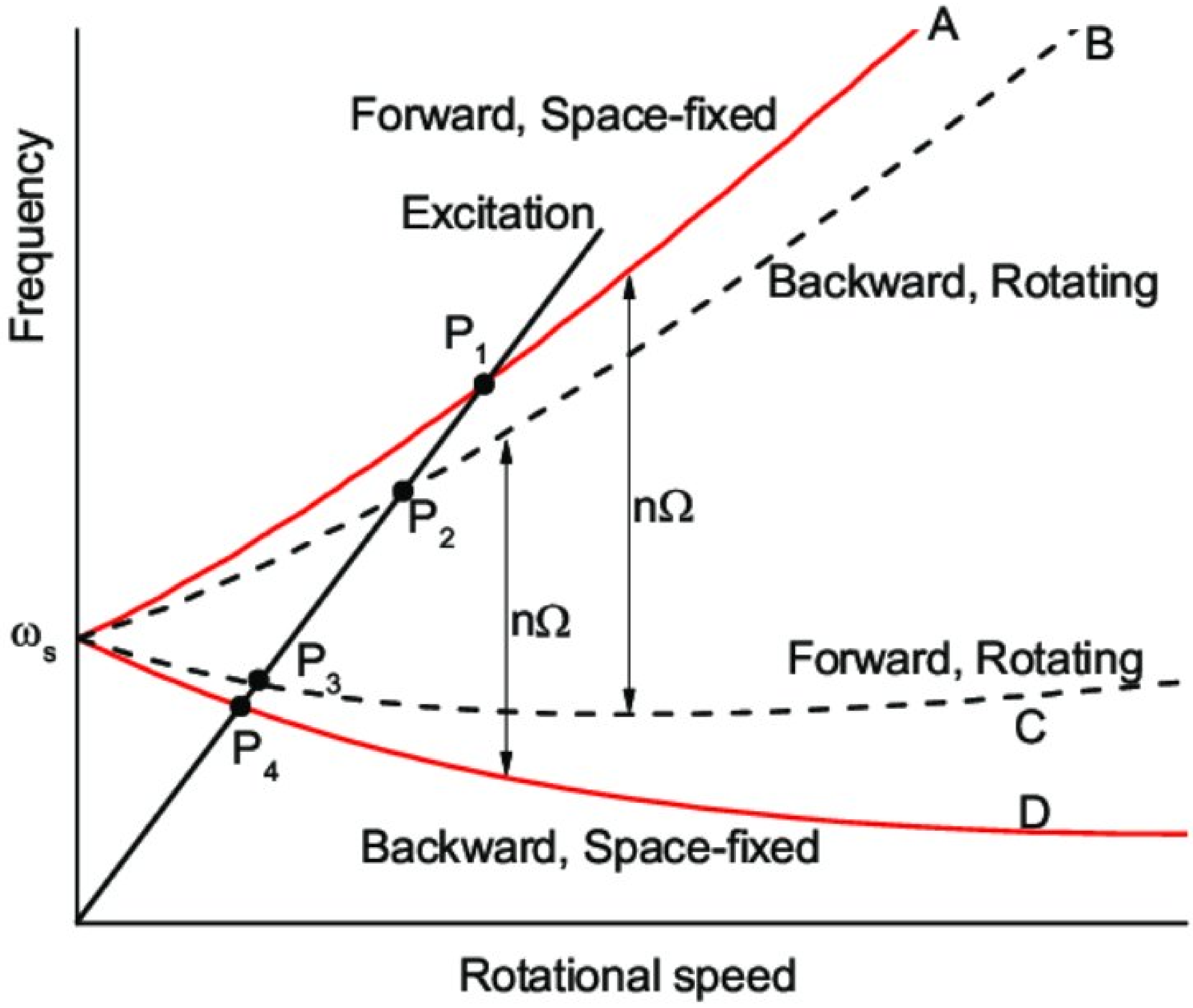

Figure 2.3: *Campbell Diagram for Frequency vs. Rotational Speed*(Lu, Tao. (2019)

2.3 Literature Study

The modal behavior of rotor systems is of great interest in many engineering applications, including aerospace, power generation, and manufacturing industries. This review aims to critically recent advancements and highlights gaps in the current body of knowledge. It follows a chronological order to showcase the evolution of research in this field and ends with a synthesis of findings and identification of areas needing further investigation. Modal analysis is crucial in the study of rotor system dynamics, particularly in assessing unbalanced effects that can induce substantial vibrations and wear on the system components. This literature review will focus on recent research related to the dynamic study of rotor systems with multi-disk systems with an unbalanced mass.

Khadem et al. (2010) investigated the principal resonances of a simply supported in-extension rotating shaft with significant amplitudes. They looked at how diametrical mass moment of inertia, eccentricity, and external damping affected the rotating shaft's steady-state response(Khadem et al., 2010).

Khadem et al. (2011) explored the two-mode combination resonances of a simply supported rotating shaft by modeling it as an in-extensional spinning beam with enormous amplitude, taking into account rotational inertia and gyroscopic effects. They used the Hamilton principle to construct the equations of motion, the harmonic balance approach to find the analytical solution, and numerical simulations to validate the results(Khadem et al., 2011).

Shahgholi and Khadem (2012a) examined the primary and parametric resonances of simply supported nonlinear rotating asymmetrical shaft with uneven mass moments of inertia and bending stiffness along the principal axis. They focused on the nonlinearities caused by stretching and huge amplitudes and used the multiple scales method to obtain the system response. They discovered that in the asymmetrical shaft, bifurcation occurs at speeds more or less than the linear forward frequency(Shahgholi & Khadem, 2012).

Shahgholi and Khadem (2012b) investigated an asymmetric rotating shaft with unequal mass moments of inertia and flexural rigidities in the primary axis. Harmonic and parametric resonances have been discussed because of nonlinearities generated by the shaft's in-extensionality and huge amplitude effects. They also investigated the stability and bifurcation of the steady-state response of a rotating asymmetrical shaft(Shahgholi & Khadem, 2012).

Shahgholi and Khadem (2012c) also investigated the simultaneous primary resonances caused by imbalance periodic force and parametric resonances caused by two sources of parametric excitations for a simply supported nonlinear spinning shaft with unequal mass moments of inertia and flexural rigidities in the principal axes. The study focused on parametric excitations such as shaft asymmetry, as well as nonlinearity caused by stretching and huge amplitudes(Shahgholi & Esmaeilzadeh Khadem, 2012).

A study by Chiu et al. (2015) investigated the dynamic behavior of a rotor system with multiple unbalanced disks using FEA. The authors developed a finite element model of the rotor system and used it to predict the natural frequencies and mode shapes of the system. The study found that the vibration characteristics of the system were affected by the number and location of the unbalanced disks. The authors also performed experimental tests on the system and compared the results with the predictions of the model. The study found good agreement between the experimental and numerical results.

A study by Ahmad Ahalmadi et al. (2018) presents a modelling and vibration analysis of a rotor with multiple disks supported by a continuous shaft for the first three nodes. The authors used the first three modes of vibration to analyze the dynamic behavior of the rotor and examine the mode shapes and natural frequencies of the system. The authors presented the results of their study, which include analyzing the effects of various parameters such as the disk diameter, and number on the vibration behavior of the rotor.

The paper "Nonlinear dynamic analysis of two-disk rotor system containing an unbalance influenced transverse crack" by Nirmal Kushwaha and V.N. Patel (2018) focuses on the analysis of a two-disk rotor system containing an unbalance influenced transverse crack using nonlinear dynamic analysis. The authors begin by discussing the importance of rotor systems in various engineering applications and the potential consequences of rotor failure. The authors note that linear models, which are commonly used for rotor analysis, have limitations when it comes to detecting cracks. The authors suggest the use of nonlinear dynamic analysis which can better capture the system's nonlinear behavior and detect cracks at early stages(Kushwaha & Patel, 2023).

In a study by Z. Hamdi Cherif and Ch. Kandouci (2020) investigates the dynamic characteristics of a multi-disk shaft system using the vectors of solution coefficients. They involved using the finite element method to develop a numerical model of the multi-disk system and simulate its dynamic behavior under different conditions. They used the vectors of solution coefficients to extract the dynamic characteristics of the system. The authors presented the results of their study, which include analyzing the effects of different parameters such as disk number, thickness and support stiffness, on the dynamic characteristics of the system. They also examined the mode shapes and natural frequencies of the system under different conditions(Cherif & Kandouci, 2020).

In a more recent study, Zhang et al. (2020) investigated the dynamic behavior of a multi-disk rotor system with multiple unbalanced disks using FEA and experimental testing. The authors developed a finite element model of the system. They also performed experimental tests on the system and compared the results with the predictions of the model. The study found that the vibration amplitudes of the system were highest at the location of the unbalanced disks and decreased as the distance from the unbalanced disks increased.

The study conducted by Xu Chen et al. (2021), investigated the unbalance vibration characteristics of a dual-rotor system through simulation. They used the finite element method to develop a numerical model of the dual-rotor system and simulate the unbalanced vibration characteristics under different conditions. They investigated the effects of different parameters, such as the unbalance magnitude, the angular position of the unbalance, and the rotor stiffness. The paper provides valuable insights into the unbalanced vibration characteristics of the dual-rotor system.

2.4 Research Gap

Despite considerable progress in the modal analysis of multi-rotor disk systems, there are still several important gaps in the literature that need to be filled. Most of the recent research has ignored the complex interaction that take place in multi-rotor configurations in favor of simpler or single-rotor systems. The complex dynamic interactions between several rotors are ignored in this simplification, despite the fact that these interactions are essential for precisely forecasting the modal properties of these systems, including their natural frequencies and mode shapes. Moreover, many previous studies make idealistic boundary conditions assumptions that are not representative of real-world applications that are not representative of real-world applications. This disparity suggests that in order to fully comprehend the impact of realistic boundary conditions on the modal behavior of multi-rotor systems, more thorough research is required that takes into account variables like support stiffness and limitations.

Further still, there is a significant lack of studies that combine both analytical and numerical methods to offer an improved understanding of modal properties of multi-rotor systems. The literature seems to use one or the other method only, with little attempt to compare methods and showcase their respective strengths and weakness. Developing hybrid methodologies that combine the accuracy of analytical methods with the versatility of numerical simulations could lead to more robust modal analysis techniques. There are other critical gaps, such as the high-frequency modes of multi-rotor systems which are just beginning to be addressed. The low to mid frequency modes are frequently examined to consider the behavior in dynamic modal fundamentals, while high-frequency modes, paramount in promoting resonance identification and safety-critical points of failure remain insufficiently addressed.

Furthermore, there is a lack of empirical support for theoretical and numerical models for multi-rotor systems, which emphasizes the need for additional experimental study to support and improve these models. Current studies frequently oversimplify or overlook the role that damping plays in affecting modal features, despite the fact that damping is essential for controlling vibrations and maintaining system stability. The influence of various damping techniques on the modal characteristics of multi-rotor systems is not well understood.

Finally, another unexplored area is the impact of cutting-edge materials and creative structural designs on the modal properties of multi-rotor systems. Investigating how these variables impact the modal features may yield important information for creating multi-rotor systems that are more dependable and efficient. By filling in these gaps, we can make significant progress in our understanding of multi-rotor disk systems' modal analysis and help create better design and analysis methods for engineering applications. Many studies in modal analysis have employed linear models that may not adequately capture the true nature of multi-rotor systems, especially when subjected to more complex configurations or boundary conditions.

Overall, this proposed study will contribute to the mathematical model for multi-rotor disk system to understand the modal behavior of rotor system.

CHAPTER THREE: METHODOLOGY

The research will be conducted under given headings.

3.1 CONCEPTUAL FRAMEWORK

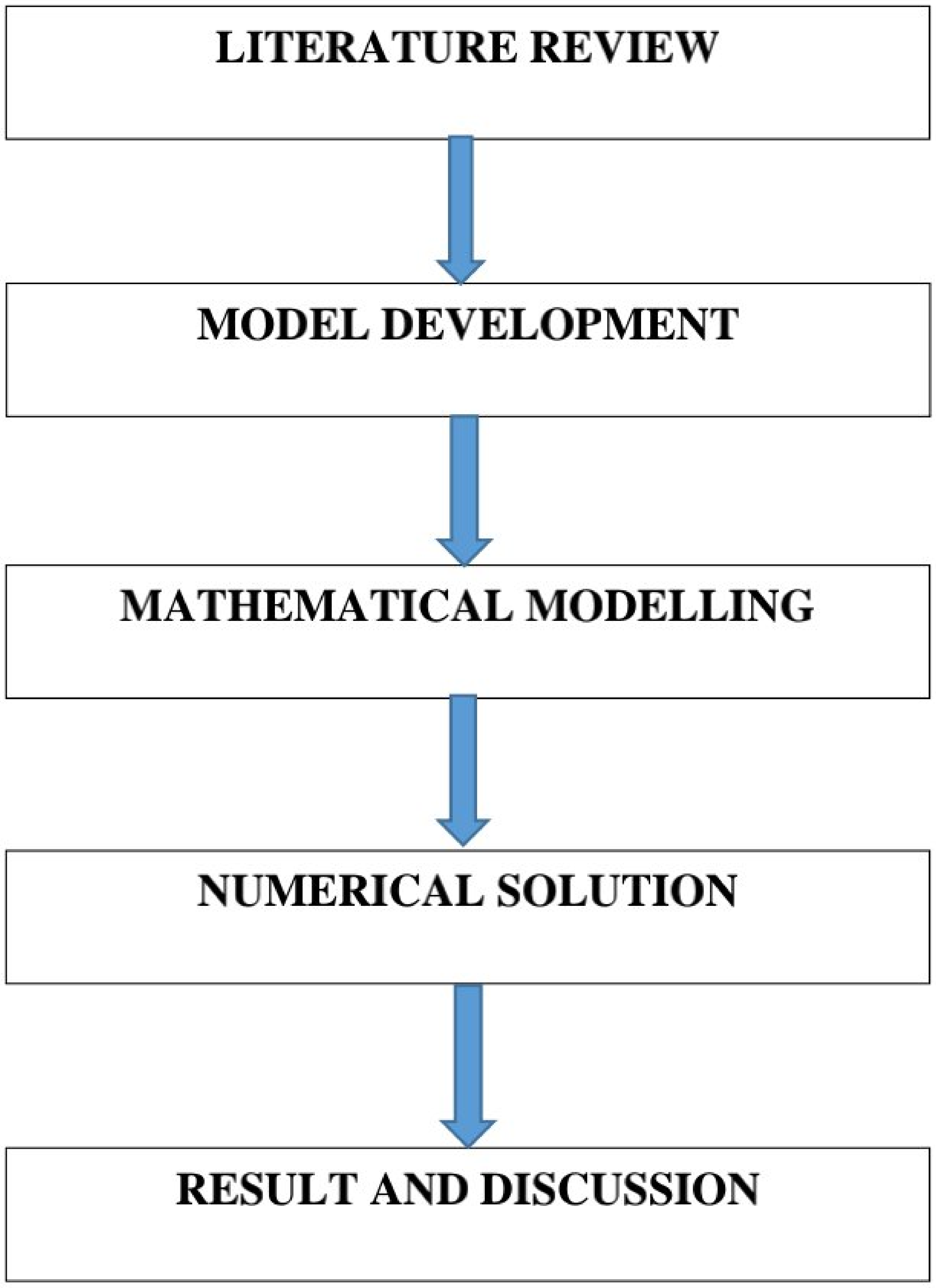

***Figure 3.1**: Methodology flow-chart for Research Process*

The methodology flow chart outlines the systematic approach adopted in this research to perform modal analysis on a multi-disk rotor system. The flow chart provides a visual summary of the sequential steps taken, from conceptual frameworks development to computational analysis and result validation. A thorough examination of the system's modal properties is made possible by the methodical planning and execution of each study step, which is ensured by this structure approach.

The key steps illustrated in the flow chart include:

1. **Conceptual Framework Development:** Initial stage where the problem is defined, and objectives are set based on literature review and theoretical understanding.
2. **Model Development:** Creating a detailed 3D model of the multi-rotor system using CATIA V5.
3. **Mathematical Modelling:** Formulating mathematical equations to represent the physical system, focusing on natural frequencies and mode shapes.
4. **Numerical Simulation:** Implementing the model in ANSYS for modal analysis to compute natural frequencies and visualize mode shapes.

3.2 Literature Review

An extensive review of the available literature reveals that modal analysis is essential for characterizing the vibrational behavior of rotor systems and for enabling their operational stability. In words, the natural frequencies and mode shapes of multi-rotor systems have been examined computationally and analytically in many studies. However, there is a noticeable gap in the detailed study of modal analysis specifically focusing on systems without imbalance, which this research aims to address. With ANSYS making it possible to accurately compute natural frequencies and mode shapes, enhancing the understanding of the system's behavior.

3.3 Model Development and Assumptions of the Model

To study the free response of the multi-disk rotor system, a theoretical model was developed using CATIA V5, a robust 3D CAD software that facilitates the precise design of complex mechanical systems. The modeling process involves creating a detailed representation of the rotor assembly including the shaft and multiple disks. The rotor-bearing system is operating at steady state condition and the damping in the rigid and isotropic bearing and seal were neglected. The shaft is assumed to be flexible, and the disk and bearing are assumed to be rigid. The longitudinal displacement in the shaft is neglected.

A detailed geometric model of the multi-rotor system is created using CATIA V5. It guarantees that the model accurately represents the geometry and material properties of the physical system by enabling the comprehensive design of mechanical parts and assemblies. Because of the sophisticated features of the CATIA V5, parametric models may be quickly created and optimized for modal analysis. The model created in CATIA V5 is used as a foundation for additional in ANSYS, where natural frequencies and mode shapes are found using modal analysis.

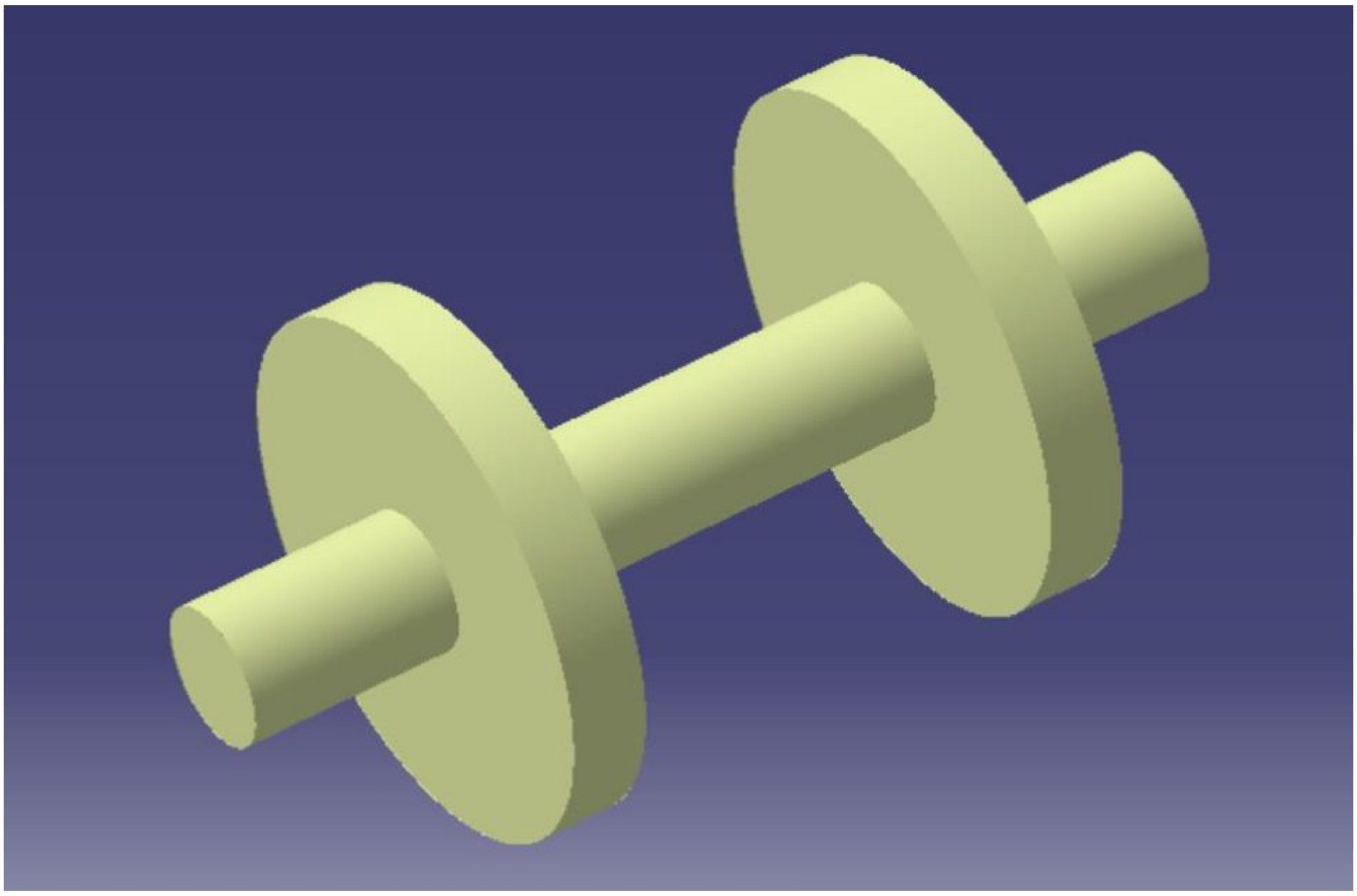

***Figure 3.2**: Assembly of shaft and multi-disk system*

3.4 Mathematical Model

The mathematical model of the multi-rotor system is based on the Euler-Bernoulli Beam Theory. For this research work, the system was assumed to consist of a rigid disk, flexible shaft and rigid, undamped, and simply supported bearings. The two disks were positioned along the length of the shaft, which was simply supported by bearings at both ends, spanning a total length of 2.12 meters. Each disk is situated at 450mm i.e., L/4 from the respective bearing on either side, resulting in a symmetrical arrangement. The distance between the centers of the disks is L/2, effectively dividing the shaft into two equal segments. The rotating shaft was modelled by rotating beam models: rotating Euler-Bernoulli beam. The Assumed Mode Method and Lagrange's equations were used to generate equations of motion for the Euler-Bernoulli Beam model, which expressed the system's kinetic and potential energies. This modelling approach can provide valuable insights into the modal behavior of thnae system and can help in designing systems that are less prone to vibration and failure. The choice of modelling method for this thesis is analytical methods(Luintel, n.d.-c).

3.5 Modal Analysis in ANSYS

ANSYS and Modal Analysis Overview:

ANSYS is a widely used popular engineering simulation software that makes it possible to model and analyze complex mechanical systems in detail. It offers a wide range of tools for carrying out finite element analysis (FEA), which is crucial for comprehending how systems behave under diverse physical circumstances. ANSYS was selected for this thesis because of its strong dynamic and vibrational analysis capabilities, which make it a perfect fit for examining the modal features of multi-rotor systems.

In engineering, modal analysis is a crucial procedure that identifies a structure's natural frequencies and mode shapes. This kind of analysis aids in determining a system's vibrational properties, which are essential for guaranteeing performance and stability. Engineers can forecast possible resonance circumstances that can result in excessive vibrations or mechanical failure by knowing the natural frequencies. In order to examine a multi-rotor system's vibrational behavior in the absence of external forces or unbalanced masses, modal analysis was used in this work.

The multi-rotor system's modal analysis is carried out using ANSYS. The program offers a thorough environment for finite element analysis, allowing for precise calculations of natural frequencies and mode shapes. After being created in CATIA V5, the model is imported into ANSYS and discretized into finite elements.

ANSYS Setup for Modal Analysis:

The natural frequencies and mode shapes of the multi-rotor system were simulated and assessed using ANSYS for the modal analysis. The multi-rotor system's 3D geometry, which was first created in CATIA V5, was imported into ANSYS to start the process. The geometry was intended to precisely replicate the physical properties of the system under study, and it comprised of a continuous shaft with two disks.

After importing the geometry, the next step was to generate the mesh. A tiny mesh was created to achieve maximum precision in the study. The mesh parameters were carefully chosen to balance computational efficiency and precision. The mesh was set with an element size of 0.02 meters, yielding 432,156 nodes and 100,018 elements. A small mesh was required in order to adequately portray the system's complex connections and dynamic behavior. The meshing procedure followed the program's default physics preferences set to mechanical and element order, ensuring that the mesh was sufficiently refined for the modal analysis.

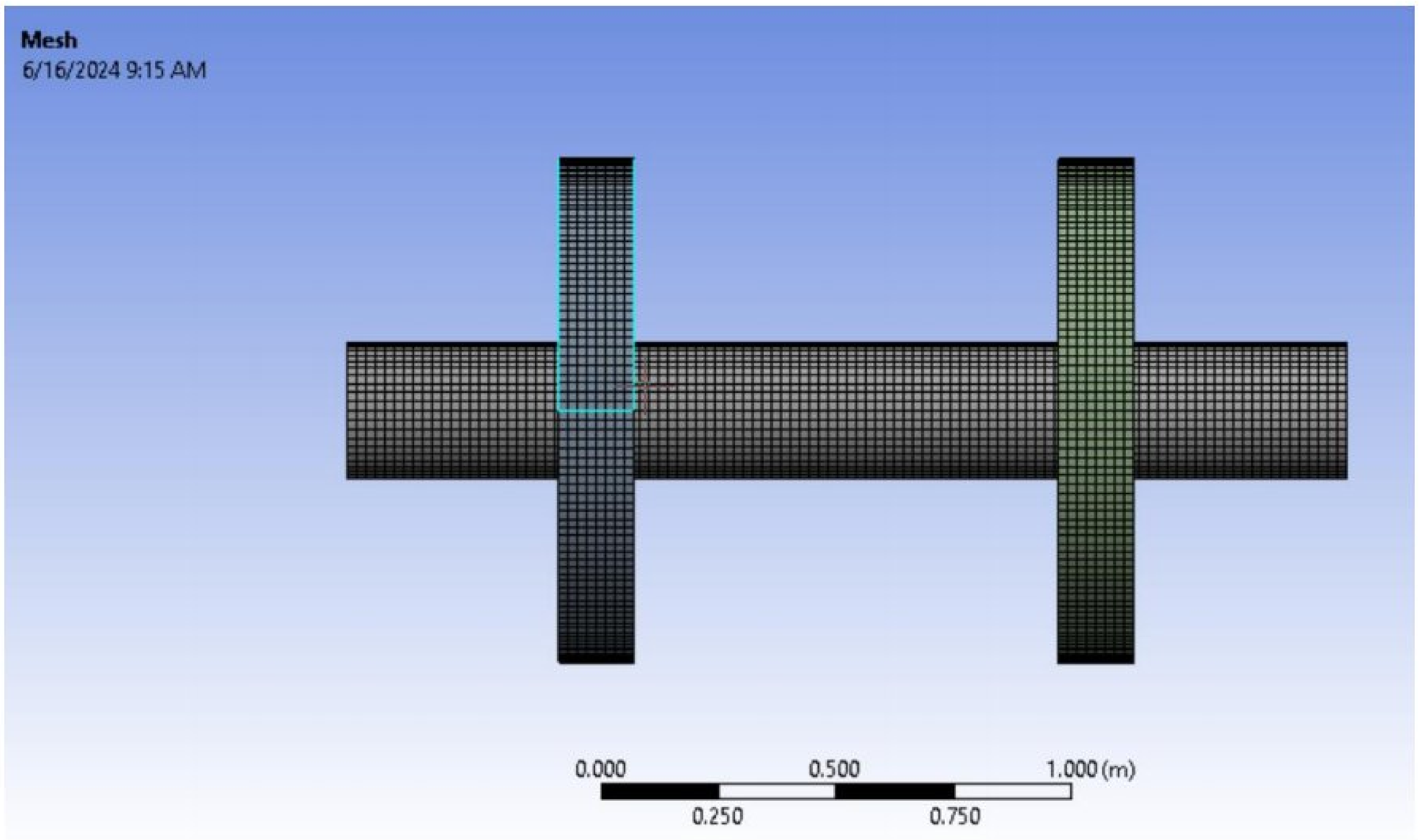

***Figure 3.3**: Meshing of Assembly (Visual representation of the meshed geometry)*

The analysis parameters were properly set up to obtain the desired modal information. The maximum number of modes to be recognized was set at six, ensuring that the major natural frequencies and mode shapes of interest were caught. The Coriolis effect was used to account for the system's rotational dynamics, which is critical for precisely modeling the behavior of spinning components. The modal analysis was then performed, and the results were used to identify the multi-rotor system's natural frequencies and related mode shapes. This extensive setup and analysis revealed crucial data about the system's vibration characteristics and potential resonance issues.

3.6 Analytical Solution of the Mathematical Model

The equations governing each model were converted into a set of ordinary differential equations. Using these equations, an analysis of free vibrations was conducted to obtain the formulas for the inherent frequencies of the system in both the forward and backward whirl directions. To interpret the analytical solutions, numerical calculations were performed according to material and geometric properties of each component of the real setup.

CHAPTER FOUR:MATHEMATICAL MODELLING AND ANALYSIS

4.1 Problem Formulation Using Euler-Bernoulli Beam Model

4.1.1 System Description

Consider the following configuration where two rigid disks are mounted on a flexible shaft, as illustrated in Figure 4.1, with the ends supported by bearings. The axes x, y and z are selected so that x is along the shaft's longitudinal direction, y is along its transverse direction on the vertical plane. Similarly, transverse displacements of every point of the shaft in horizontal and vertical directions are denoted by $v(x, t)$ and $w(x, t)$. Materials parameters of the shaft-rotor system include Elasticity (E) and density (ρ), as well as cross sectional properties area (A).

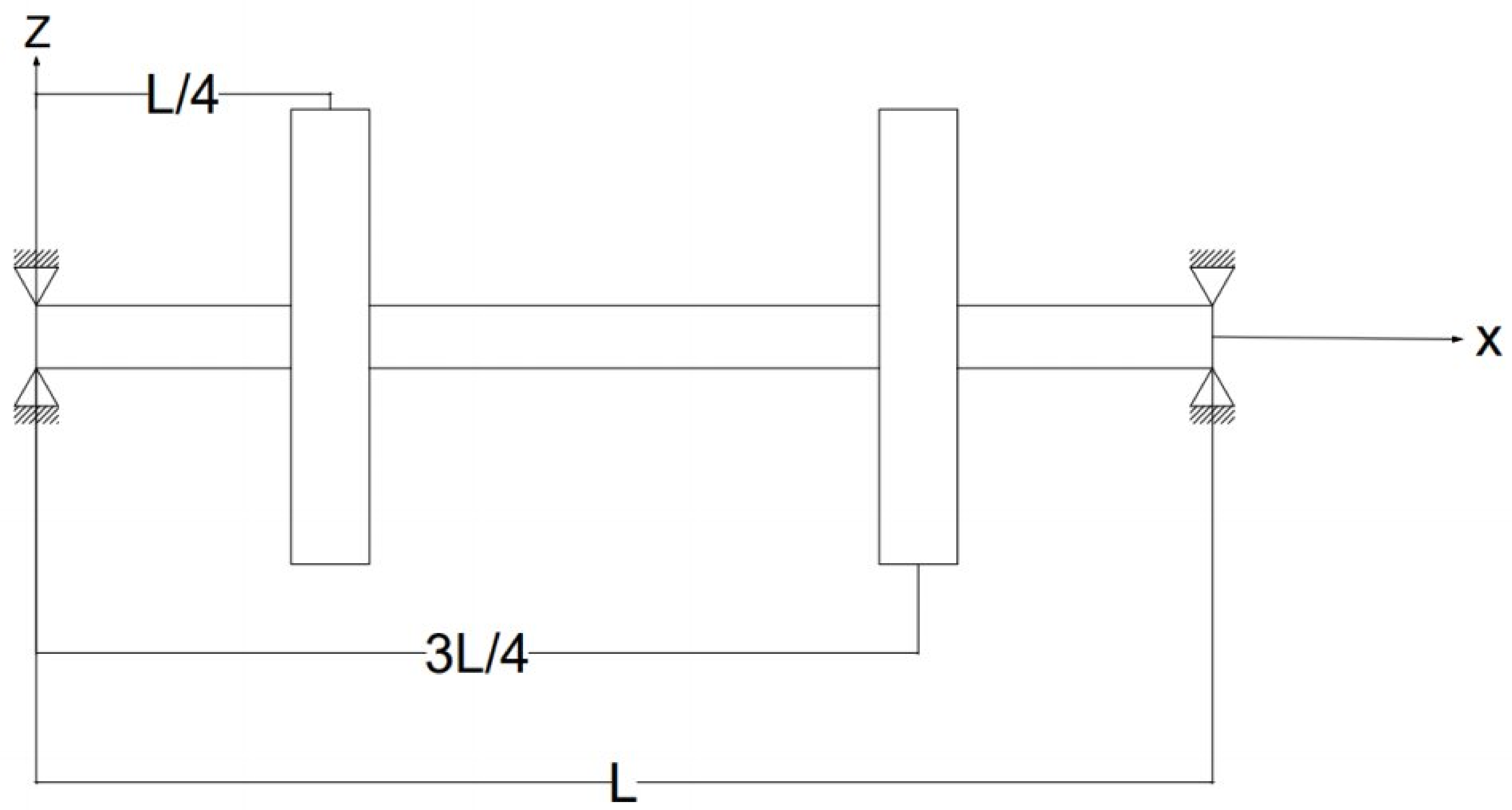

Figure 4.1: *Shaft-Disks 2D Design*

4.1.2 System Kinematics

Figure depicts a schematic of a spinning flexible shaft and rigid disk system arrangement. The shaft spins about an axis x with constant angular velocity Ω relative t inertial axes xyz. The axes y and z rotate together with body at the same angular velocity Ω round the axis x. The bending orientations of the shaft at every point of its neutral axis can be written as $v(x,t)$ and $w(x,t)$ along y and z, respectively.

The angular velocity vector and the neutral's position vector can be represented in vector form as below:(Khanlo et al., 2011)

$$\boldsymbol{\omega_s} = [\boldsymbol{\Omega}\ \ \mathbf{0}\ \ \mathbf{0}] \tag{4.1}$$

$$\boldsymbol{r_s} = \boldsymbol{vj} + \boldsymbol{wk} \tag{4.2}$$

The velocity of every point on the shaft's neutral axis with respect to inertial frame (Khanlo et al., 2011) is given by

$$\boldsymbol{v_s} = \dot{\boldsymbol{v}}\boldsymbol{j} + \dot{\boldsymbol{w}}\boldsymbol{k} + \boldsymbol{\Omega i} \times (\boldsymbol{vj} + \boldsymbol{wk}) = (\dot{\boldsymbol{v}} - \boldsymbol{\Omega w})\boldsymbol{j} + (\dot{\boldsymbol{w}} + \boldsymbol{\Omega v})\boldsymbol{k} \tag{4.3}$$

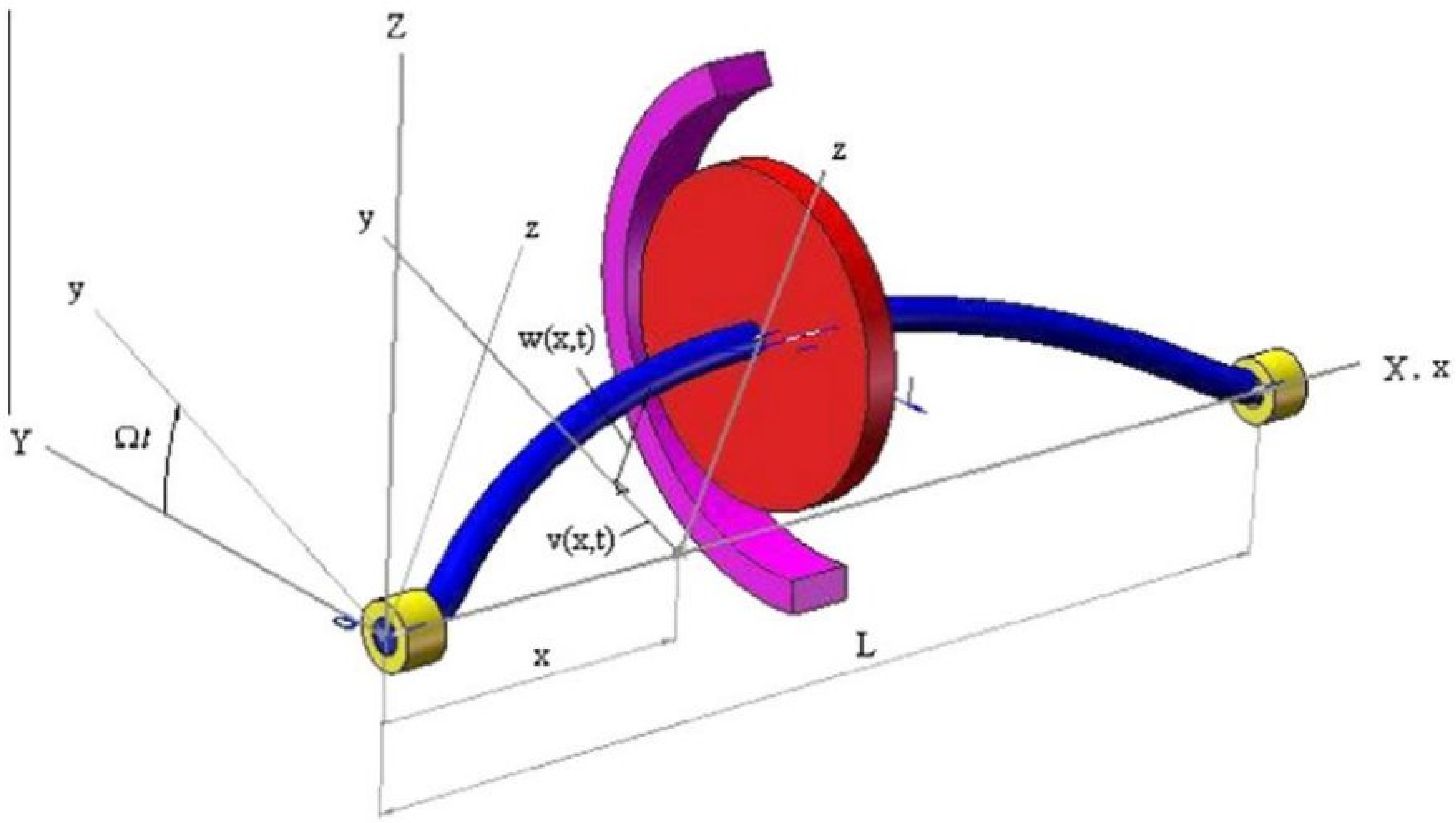

Figure 4.2: *Rotating Shaft-Disk system in distorted state* (Khanlo et al., 2011)

The angular speed vector for the disk is presented as: (Khanlo et al., 2011):

$$\boldsymbol{\omega_d} = \left(\boldsymbol{\Omega} + \boldsymbol{v}'\dot{\boldsymbol{w}}'\right)\boldsymbol{i} + (-\boldsymbol{\Omega v}' + \dot{\boldsymbol{w}}')\boldsymbol{j} + (\boldsymbol{\Omega w}' + \dot{\boldsymbol{v}}')\boldsymbol{k} \tag{4.4}$$

4.1.3 Kinetic and Strain Energy of the Rotating Shaft-Disk System

The rotating shaft's kinetic energy is expressed is as:

$$T_s = \frac{1}{2}\rho A \int_0^L [(\dot{v} - \Omega w)^2 + (\dot{w} + \Omega v)^2]dx + \frac{1}{2}\rho J_{ps} \int_0^L [(\Omega + v'\dot{w}')^2]dx +$$

$$\frac{1}{2}\rho I_s \int_0^L [(-\Omega v' - \dot{w}')^2 + (-\Omega w' + \dot{v}')^2]dx \tag{4.5}$$

Avoiding the higher order terms, Kinetic Energy of the shaft given by Eq (4.5) can be expressed as

$$\begin{aligned} T_s = {} & \frac{1}{2}\rho A \int_0^L \dot{v}^2 dx + \frac{1}{2}\rho A \int_0^L \dot{w}^2 dx + \frac{1}{2}\rho A \Omega^2 \int_0^L v^2 dx + \frac{1}{2}\rho A \Omega^2 \int_0^L w^2 dx \\ & + \rho A \Omega \int_0^L \dot{w} v \, dx - \rho A \Omega \int_0^L \dot{v} w dx + \frac{1}{2}\rho J_{ps} \Omega^2 L + \rho J_{ps} \Omega \int_0^L \dot{w}' v' \, dx \\ & + \frac{1}{2}\rho I_s \int_0^L (\dot{v}')^2 \, dx + \frac{1}{2}\rho I_s \int_0^L (\dot{w}')^2 \, dx + \frac{1}{2}\rho I_s \Omega^2 \int_0^L v'^2 \, dx \\ & + \frac{1}{2}\rho I_s \Omega^2 \int_0^L w'^2 \, dx + \rho I_s \Omega \int_0^L \dot{w}' v' \, dx - \rho I_s \Omega \int_0^L \dot{v}' w' \, dx \end{aligned} \tag{4.6}$$

Similarly, the Kinetic Energy expression of a rigid disk has the form.

$$\begin{aligned} T_d = {} & \frac{1}{2}\big[M_1\{(\dot{v} - \Omega w)^2 + (\dot{w} + \Omega v)^2\} \\ & + h\rho\big\{I_{y1}(\Omega v' + \dot{w}')^2 + I_{z1}(-\Omega w' + \dot{v}')^2 + J_{p1}(\Omega + v'\dot{w}')^2\big\}\big]\Big|_{x=\frac{L}{4}} \\ & + \frac{1}{2}\big[M_2\{(\dot{v} - \Omega w)^2 + (\dot{w} + \Omega v)^2\} \\ & + h\rho\big\{I_{y2}(\Omega v' + \dot{w}')^2 + I_{z2}(-\Omega w' + \dot{v}')^2 + J_{p2}(\Omega + v'\dot{w}')^2\big\}\big]\Big|_{x=\frac{3L}{4}} \end{aligned} \tag{4.7}$$

$$T_d = \frac{1}{2}M_1(\dot{v})^2\Big|_{x=\frac{L}{4}} + \frac{1}{2}M_1(\dot{w})^2\Big|_{x=\frac{L}{4}} + \frac{1}{2}M_1\Omega^2(v)^2\Big|_{x=\frac{L}{4}} + \frac{1}{2}M_1\Omega^2(w)^2\Big|_{x=\frac{L}{4}}$$
$$+ M_1\Omega(\dot{w}v)\Big|_{x=\frac{L}{4}} - M_1\Omega(\dot{v}w)\Big|_{x=\frac{L}{4}} + \frac{1}{2}\rho_1 hJ_{p1}\Omega^2 + \rho_1 hJ_{p1}\Omega(\dot{w}'v')\Big|_{x=\frac{L}{4}}$$
$$+ \frac{1}{2}\rho_1 hI_1(\dot{v}')^2\Big|_{x=\frac{L}{4}} + \frac{1}{2}\rho_1 hI_1(\dot{w}')^2\Big|_{x=\frac{L}{4}} + \frac{1}{2}\rho_1 hI_1\Omega^2(v')^2\Big|_{x=\frac{L}{4}}$$
$$+ \frac{1}{2}\rho_1 hI_1\Omega^2(w')^2\Big|_{x=\frac{L}{4}} + \rho_1 hI_1\Omega(\dot{w}'v')\Big|_{x=\frac{L}{4}} - \rho_1 hI_1\Omega(\dot{v}'w')\Big|_{x=\frac{L}{4}}$$
$$+ \frac{1}{2}M_2(\dot{v})^2\Big|_{x=\frac{3L}{4}} + \frac{1}{2}M_2(\dot{w})^2\Big|_{x=\frac{3L}{4}} + \frac{1}{2}M_2\Omega^2(v)^2\Big|_{x=\frac{3L}{4}}$$
$$+ \frac{1}{2}M_2\Omega^2(w)^2\Big|_{x=\frac{3L}{4}} + M_2\Omega(\dot{w}v)\Big|_{x=\frac{3L}{4}} - M_2\Omega(\dot{v}w)\Big|_{x=\frac{3L}{4}}$$
$$+ \frac{1}{2}\rho_2 hJ_{p2}\Omega^2 + \rho_2 hJ_{p2}\Omega(\dot{w}'v')\Big|_{x=\frac{3L}{4}} + \frac{1}{2}\rho_2 hI_2(\dot{v}')^2\Big|_{x=\frac{3L}{4}}$$
$$+ \frac{1}{2}\rho_2 hI_2(\dot{w}')^2\Big|_{x=\frac{3L}{4}} + \frac{1}{2}\rho_2 hI_2\Omega^2(v')^2\Big|_{x=\frac{3L}{4}} + \frac{1}{2}\rho_2 hI_2\Omega^2(w')^2\Big|_{x=\frac{3L}{4}}$$
$$+ \rho_2 hI_2\Omega(\dot{w}'v')\Big|_{x=\frac{3L}{4}} - \rho_2 hI_2\Omega(\dot{v}'w')\Big|_{x=\frac{3L}{4}}$$

(4.8)

As the shaft had a circular cross-section, the polar moment of inertia is double that of its diametral moment of inertia, and the same is true for the disk. The system's total kinetic energy is the sum of T_s and T_d.

The strain energy on a shaft caused by bending has the form

$$\boldsymbol{U_s = \frac{1}{2}EI_s\int_0^L[(v'')^2 + (w'')^2]dx} \qquad (4.9)$$

Work done by the Harmonic force is given by

$$\boldsymbol{W_{ext} = F(t)(v)\Big|_{x=\frac{L}{4}}} \qquad (4.10)$$

4.1.4 Equation of Motion

To obtain the motion equations, use the assumed mode approach and specify displacements as:

$$v(x,t) = \{\phi(x)\}^T\{q_v(t)\} = \phi^T(x)q_v(t) \qquad (4.11)$$

$$w(x,t) = \{\phi(x)\}^T\{q_w(t)\} = \phi^T(x)q_w(t) \qquad (4.12)$$

where $\phi(x)$ is the acceptable spatial function vector that specifies the shaft's transverse deflections, and the superscript T represents the transpose of a matrix or vector. The column vectors $\phi(x), q_v(t)$, and $q_w(t)$ represent time-dependent generalized coordinates.

Substituting v and w into Eq (4.6), the expression for kinetic energy of the shaft can be obtained as

$$
\begin{aligned}
T_s = \frac{1}{2}\rho A \int_0^L (\phi \dot{q_v})^2 dx \\
&+ \frac{1}{2}\rho A \int_0^L (\phi \dot{q_w})^2 dx + \frac{1}{2}\rho A \Omega^2 \int_0^L (\phi q_v)^2 dx + \frac{1}{2}\rho A \Omega^2 \int_0^L (\phi q_w)^2 dx \\
&+ \rho A \Omega \int_0^L (\phi^2 q_v \dot{q_w})\, dx - \rho A \Omega \int_0^L (\phi^2 \dot{q_v} q_w) dx + \frac{1}{2}\rho J_{ps} \Omega^2 L \\
&+ \rho J_{ps} \Omega \int_0^L (\phi')^2 q_v \dot{q_w}\, dx + \frac{1}{2}\rho I_s \int_0^L (\phi' \dot{q_v})^2\, dx \\
&+ \frac{1}{2}\rho I_s \int_0^L (\phi' \dot{q_w})^2\, dx + \frac{1}{2}\rho I_s \Omega^2 \int_0^L (\phi' q_v)^2\, dx \\
&+ \frac{1}{2}\rho I_s \Omega^2 \int_0^L (\phi' q_w)^2\, dx + \rho I_s \Omega \int_0^L (\phi')^2 q_v \dot{q_w}\, dx \\
&- \rho I_s \Omega \int_0^L (\phi')^2 \dot{q_v} q_w\, dx
\end{aligned}
\tag{4.13}
$$

Similarly, substituting v and w into Eq (4.8), the expression for Kinetic Energy of the disks can be obtained as

$$
\begin{aligned}
T_d &= \tfrac{1}{2}M_1(\phi\dot{q_v})^2\big|_{x=\frac{L}{4}} + \tfrac{1}{2}M_1(\phi\dot{q_w})^2\big|_{x=\frac{L}{4}} + \tfrac{1}{2}M_1\Omega^2(\phi q_v)^2\big|_{x=\frac{L}{4}} + \\
&\tfrac{1}{2}M_1\Omega^2(\phi q_v)^2\big|_{x=\frac{L}{4}} + M_1\Omega(\phi^2 q_v\dot{q_w})\big|_{x=\frac{L}{4}} - M_1\Omega(\phi^2\dot{q_v}q_w)\big|_{x=\frac{L}{4}} + \tfrac{1}{2}\rho_1 h J_{p1}\Omega^2 + \\
&\rho_1 h J_{p1}\Omega((\phi')^2 q_v\dot{q_w})\big|_{x=\frac{L}{4}} + \tfrac{1}{2}\rho_1 h I_1(\phi'\dot{q_v})^2\big|_{x=\frac{L}{4}} + \tfrac{1}{2}\rho_1 h I_1(\phi'\dot{q_w})^2\big|_{x=\frac{L}{4}} + \\
&\tfrac{1}{2}\rho_1 h I_1\Omega^2(\phi' q_v)^2\big|_{x=\frac{L}{4}} + \tfrac{1}{2}\rho_1 h I_1\Omega^2(\phi' q_w)^2\big|_{x=\frac{L}{4}} + \rho_1 h I_1\Omega(\phi')^2 q_v\dot{q_w}\big|_{x=\frac{L}{4}} - \\
&\rho_1 h I_1\Omega(\phi')^2\dot{q_v}q_w\big|_{x=\frac{L}{4}} + \tfrac{1}{2}M_2(\phi\dot{q_v})^2\big|_{x=\frac{3L}{4}} + \tfrac{1}{2}M_2(\phi\dot{q_w})^2\big|_{x=\frac{3L}{4}} + \\
&\tfrac{1}{2}M_2\Omega^2(\phi q_v)^2\big|_{x=\frac{3L}{4}} + \tfrac{1}{2}M_2\Omega^2(\phi q_v)^2\big|_{x=\frac{3L}{4}} + M_2\Omega(\phi^2 q_v\dot{q_w})\big|_{x=\frac{3L}{4}} - \\
&M_2\Omega(\phi^2\dot{q_v}q_w)\big|_{x=\frac{3L}{4}} + \tfrac{1}{2}\rho_2 h J_{p2}\Omega^2 + \rho_2 h J_{p2}\Omega((\phi')^2 q_v\dot{q_w})\big|_{x=\frac{3L}{4}} +
\end{aligned}
$$

$$\frac{1}{2}\rho_2 hI_2(\phi'\dot{q_v})^2\Big|_{x=\frac{3L}{4}} + \frac{1}{2}\rho_2 hI_2(\phi'\dot{q_w})^2\Big|_{x=\frac{3L}{4}} + \frac{1}{2}\rho_2 hI_2\Omega^2(\phi' q_v)^2\Big|_{x=\frac{3L}{4}} +$$

$$\frac{1}{2}\rho_2 hI_2\Omega^2(\phi' q_w)^2\Big|_{x=\frac{3L}{4}} + \rho_2 hI_2\Omega(\phi')^2 q_v\dot{q_w}\Big|_{x=\frac{3L}{4}} - \rho_2 hI_2\Omega(\phi')^2\dot{q_v}q_w\Big|_{x=\frac{3L}{4}}$$

(4.14)

Similarly, substituting v and w into Eq (4.9), the expression for Strain Energy of the shaft can be obtained as

$$U_s = \frac{1}{2}EI_s\int_0^L[(\phi'' q_v)^2 + (\phi'' q_w)^2]dx \tag{4.15}$$

Finally, substituting v and w into Eq (4.10), the expression for the work done by the harmonic force can be obtained as

$$W_{ext} = F(t)(\phi q_v)\Big|_{x=\frac{L}{4}} \tag{4.16}$$

Using Lagrange's Equation,

$$\frac{d}{dt}\left(\frac{\partial T}{\partial \dot{q}}\right) - \frac{\partial T}{\partial q} + \frac{\partial U}{\partial q} - \frac{\partial W_{ext}}{\partial q} = 0 \tag{4.17}$$

The application of Lagrange's Equation and after certain adjustments, yields modified equations of motion for transverse vibrations respectively as

$$\begin{gathered}
\rho A\ddot{q_v}\int_0^L \phi^2 dx + \rho I_s\ddot{q_v}\int_0^L(\phi')^2 dx + M_1\ddot{q_v}\phi^2\Big|_{x=\frac{L}{4}} + \rho_1 hI_1\ddot{q_v}(\phi')^2\Big|_{x=\frac{L}{4}} + \\
M_2\ddot{q_v}\phi^2\Big|_{x=\frac{3L}{4}} + \rho_2 hI_2\ddot{q_v}(\phi')^2\Big|_{x=\frac{3L}{4}} - 2\rho A\Omega\dot{q_w}\int_0^L \phi^2\, dx - 2\rho I_s\Omega\dot{q_w}\int_0^L(\phi')^2\, dx - \\
2M_1\Omega\dot{q_w}\phi^2\Big|_{x=\frac{L}{4}} - 2\rho_1 hI_1\Omega\dot{q_w}(\phi')^2\Big|_{x=\frac{L}{4}} - 2M_2\Omega\dot{q_w}\phi^2\Big|_{x=\frac{3L}{4}} - \\
2\rho_2 hI_2\Omega\dot{q_w}(\phi')^2\Big|_{x=\frac{3L}{4}} - \rho J_{ps}\Omega\dot{q_w}\int_0^L(\phi')^2\, dx - \rho_1 hJ_{p1}\Omega\dot{q_w}(\phi')^2\Big|_{x=\frac{L}{4}} - \\
\rho_2 hJ_{p2}\Omega\dot{q_w}(\phi')^2\Big|_{x=\frac{3L}{4}} - \rho A\Omega^2 q_v\int_0^L \phi^2\, dx - \rho I_s\Omega^2 q_v\int_0^L(\phi')^2\, dx - \\
M_1\Omega^2\phi^2 q_v\Big|_{x=\frac{L}{4}} - \rho_1 hI_1\Omega^2 q_v(\phi')^2\Big|_{x=\frac{L}{4}} - M_2\Omega^2\phi^2 q_v\Big|_{x=\frac{3L}{4}} - \rho_2 hI_2\Omega^2 q_v(\phi')^2\Big|_{x=\frac{3L}{4}} + \\
EI_s q_v\int_0^l(\phi'')^2\, dx - F(t)\phi_1\Big|_{x=\frac{L}{4}} = 0
\end{gathered} \tag{4.18}$$

$$\rho A\ddot{q_w}\int_0^L \phi^2 dx + \rho I_s\ddot{q_w}\int_0^L(\phi')^2 dx + M_1\ddot{q_w}\phi^2\Big|_{x=\frac{L}{4}} + \rho_1 hI_1\ddot{q_w}(\phi')^2\Big|_{x=\frac{L}{4}} +$$

$$M_2\ddot{q_w}\phi^2\Big|_{x=\frac{3L}{4}} + \rho_2 hI_2\ddot{q_w}(\phi')^2\Big|_{x=\frac{3L}{4}} - 2\rho A\Omega\dot{q_v}\int_0^L \phi^2\, dx - 2\rho I_s\Omega\dot{q_v}\int_0^L(\phi')^2\, dx -$$

$$2M_1\Omega\dot{q_v}\phi^2\Big|_{x=\frac{L}{4}} - 2\rho_1 hI_1\Omega\dot{q_v}(\phi')^2\Big|_{x=\frac{L}{4}} - 2M_2\Omega\dot{q_v}\phi^2\Big|_{x=\frac{3L}{4}} - 2\rho_2 hI_2\Omega\dot{q_v}(\phi')^2\Big|_{x=\frac{3L}{4}} -$$

$$\rho J_{ps}\Omega\dot{q_v}\int_0^L(\phi')^2\,dx - \rho_1 hJ_{p1}\Omega\dot{q_v}(\phi')^2\Big|_{x=\frac{L}{4}} - \rho_2 hJ_{p2}\Omega\dot{q_v}(\phi')^2\Big|_{x=\frac{3L}{4}} -$$

$$\rho A\Omega^2 q_v\int_0^L\phi^2\,dx - \rho I_s\Omega^2 q_w\int_0^L(\phi')^2\,dx - M_1\Omega^2\phi^2 q_w\Big|_{x=\frac{L}{4}} -$$

$$\rho_1 hI_1\Omega^2 q_w(\phi')^2\Big|_{x=\frac{L}{4}} - M_2\Omega^2\phi^2 q_w\Big|_{x=\frac{3L}{4}} - \rho_2 hI_2\Omega^2 q_w(\phi')^2\Big|_{x=\frac{3L}{4}} +$$

$$EI_s q_w\int_0^l(\phi'')^2\,dx = 0 \qquad (4.19)$$

4.1.5 System's Response and Discretization of its Equation

For the assumed mode method, it can be assumed that

For 1st transverse mode,

$$\phi(x) = sin\left(\frac{\pi x}{L}\right)$$

(4.20)

$$\phi' = \frac{\pi}{L}cos\left(\frac{\pi x}{L}\right)$$

$$\phi'' = \frac{-\pi^2}{L^2}sin\left(\frac{\pi x}{L}\right)$$

Substituting the Eq (4.20) into the equations (4.18) and (4.19)

A system of linear ordinary differential equations for assumed mode can be obtained as

$$M_i\ddot{q}_{v_i}(t) - C_i\dot{q}_{w_i}(t) + K_i q_{v_i}(t) = F_i(t) \qquad (4.21)$$

$$M_i\ddot{q}_{w_i}(t) + C_i\dot{q}_{v_i}(t) + K_i q_{w_i}(t) = 0 \qquad (4.22)$$

where,

$$M_i = \frac{1}{2}\rho AL + \frac{\pi^2}{2L}\rho I_S + \frac{M_1}{2} + \frac{\pi^2}{2L^2}\rho_1 hI_2 + \frac{M_2}{2} + \frac{\pi^2}{2L^2}\rho_2 hI_2 \qquad (4.23)$$

$$C_i = \rho AL\Omega + \frac{\pi^2}{L}\rho I_S\Omega + M_1\Omega + \frac{\pi^2}{L^2}\rho_1 hI_1\Omega + \frac{\pi^2}{2L}\rho J_{PS}\Omega + \frac{\pi^2}{2L^2}\rho_1 hJ_{P1}\Omega + M_G\Omega + \frac{\pi^2}{L^2}\rho_2 hI_2\Omega + \frac{\pi^2}{2L^2}\rho_2 hJ_{P2}\Omega$$

(4.24)

$$K_i = \frac{\pi^4}{2L^3} EI_S - \frac{1}{2}\rho AL\Omega^2 - \frac{\pi^2}{2L}\rho I_S\Omega^2 - \frac{M_1}{2}\Omega^2 - \frac{\pi^2}{2L^2}\rho_1 hI_1\Omega^2 - \frac{M_2}{2}\Omega^2 - \frac{\pi^2}{2L^2}\rho_2 hI_2\Omega^2 \quad (4.25)$$

$$F_i = \frac{F(t)}{\sqrt{2}} \quad (4.26)$$

where,

M_i = Modal Mass

C_i = Modal damping due to gyroscopic effect

K_i = Modal Stiffness

F_i = Modal Force of the system

4.1.6 Solution of the System for Free Response

Equations (4.21) and (4.20) for free vibration analysis decrease to given below equations when $F(t) = 0$ is substituted.

$$M_i \ddot{q_{v_i}}(t) - C_i \dot{q_{w_i}}(t) + K_i q_{v_i}(t) = 0 \quad (4.27)$$

$$M_i \ddot{q_{w_i}}(t) + C_i \dot{q_{v_i}}(t) + K_i q_{w_i}(t) = 0 \quad (4.28)$$

Substituting

$$q_v(t) = \overline{q_v} e^{\lambda_i t} \quad (4.29)$$

and

$$q_w(t) = \overline{q_v} e^{\lambda_i t} \quad (4.30)$$

into Equations (4.27) and (4.28), we obtain the system's characteristics equation as:

$$M_i {\lambda_i}^4 + \left({C_i}^2 + 2K_i M_i\right){\lambda_i}^2 + {k_i}^2 = 0 \quad (4.31)$$

Eq (4.31) is quadratic on ${\lambda_i}^2$ and its roots are given as

$${\lambda_1}^2 = \frac{-1}{2}\left[\left\{\left(\frac{C_i}{M_i}\right)^2 + \frac{2K_i}{M_i}\right\} - \sqrt{\left(\frac{C_i}{M_i}\right)^4 + 4\left(\frac{C_i}{M_i}\right)^2 \frac{K_i}{M_i}}\right] \quad (4.32)$$

$$\lambda_2{}^2 = \frac{-1}{2}\left[\left\{\left(\frac{C_i}{M_i}\right)^2 + \frac{2K_i}{M_i}\right\} + \sqrt{\left(\frac{C_i}{M_i}\right)^4 + 4\left(\frac{C_i}{M_i}\right)^2 \frac{K_i}{M_i}}\right] \tag{4.33}$$

Next, the natural frequencies for the backward whirl and forward whirl are provided, respectively, by:

$$(\lambda|i)_1 = \sqrt{\frac{1}{2}\left[\left\{\left(\frac{C_i}{M_i}\right)^2 + \frac{2K_i}{M_i}\right\} - \sqrt{\left(\frac{C_i}{M_i}\right)^4 + 4\left(\frac{C_i}{M_i}\right)^2 \frac{K_i}{M_i}}\right]} \tag{4.34}$$

$$(\lambda|i)_2 = \sqrt{\frac{1}{2}\left[\left\{\left(\frac{C_i}{M_i}\right)^2 + \frac{2K_i}{M_i}\right\} + \sqrt{\left(\frac{C_i}{M_i}\right)^4 + 4\left(\frac{C_i}{M_i}\right)^2 \frac{K_i}{M_i}}\right]} \tag{4.35}$$

4.2 Modal Analysis of the System

The natural frequencies and associated mode shapes of the multirotor system were determined using the modal analysis. This research is critical for understanding the system's vibrational characteristics, which can guide design decisions to avoid resonance and assure stability.

4.2.1 First Transverse Mode of Multi-Rotor System

The graphic below depicts the initial transverse mode of the multi-rotor system as determined by ANSYS's modal analysis software.

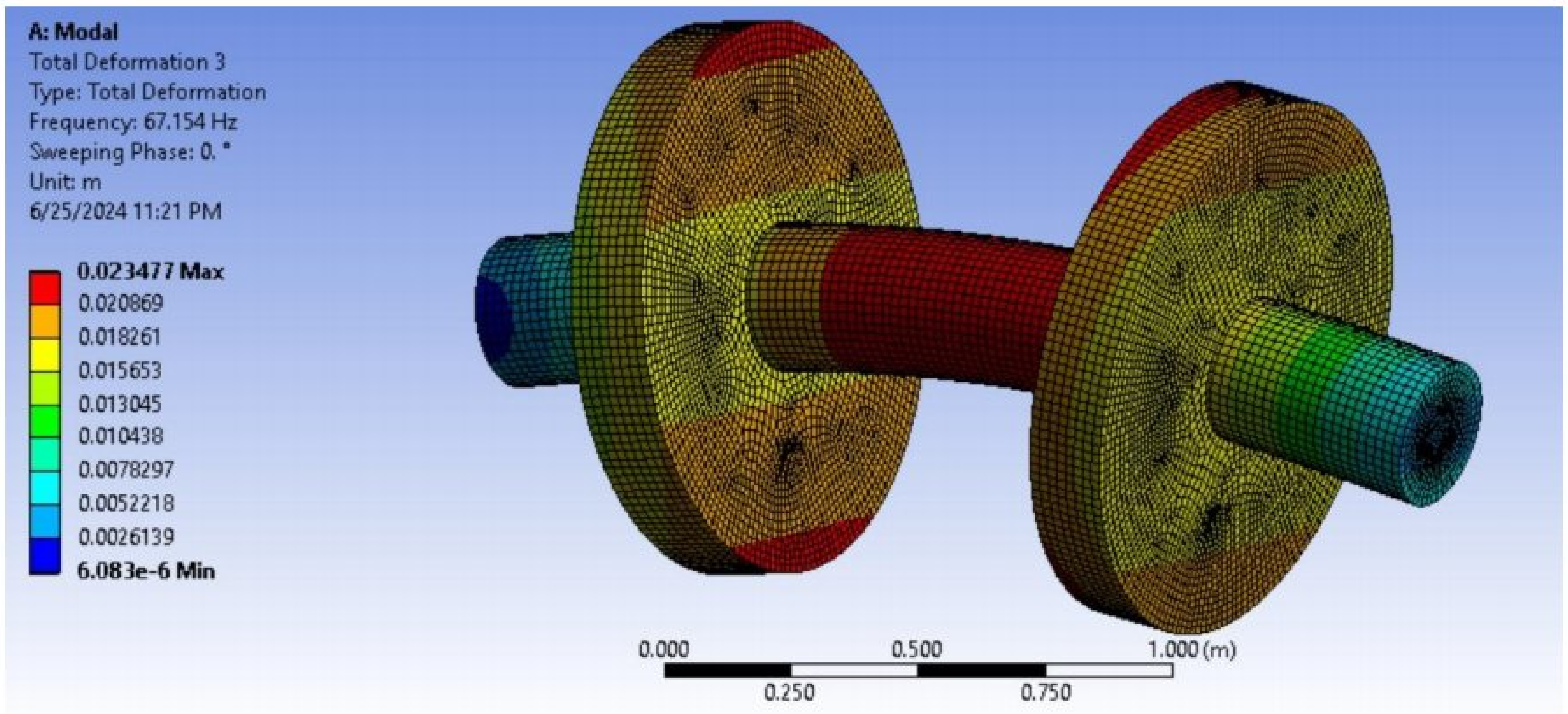

Figure 4.3: *First transverse mode of the multi-rotor system*

Figure 4.3 depicts the initial transverse mode of the multi-rotor system, with entire deformation occurring at a frequency of 67.154 Hz. Color gradients are used to depict the deformation, with red indicating highest distortion and blue indicating least deformation.

Description and Analysis:

The modal analysis reveals the first transverse mode, which occurs at a frequency of 67.154 Hz. This model is distinguished by the rotor system bending in a transverse direction relative to its longitudinal axis. The color gradient in the figure emphasizes the areas of maximum deformation (red) and minimum deformation (blue), which are crucial for understanding the system's dynamic response under operational conditions.

This mode shape suggests possible areas of significant stress, notably at the disk margins and shaft regions where maximal deformation occurs. Identifying these locations is critical for maximizing the design's longevity and performance of the rotor system. The first transverse mode gives information on the system's inherent behavior, which can be utilized to predict and minimize resonant conditions that may occur during operation.

The results of the modal analysis will be used to enhance the system design such that the operational frequencies avoid these crucial natural frequencies, lowering the danger of resonance and mechanical failure.

CHAPTER FIVE: RESULTS AND DISCUSSION

5.1 Numerical Findings and a Discussion for the Euler-Bernoulli Beam Model

In the following numerical examples, the corresponding parameters are chosen as shown in **Table 5.1.**

Table 5.1: *Parameters of the Shaft Rotor system for Euler Bernoulli Model*

PARAMETERS	VALUE
Density of Shaft material, ρ	7750 kg/m^3
Density of Disk 1 material, ρ_1	7750 kg/m^3
Density of Disk 2 material, ρ_2	7750 kg/m^3
Length of the Shaft, L	2.12 m
Cross sectional area of shaft, A	0.066 m^2
Modulus of Elasticity of shaft and disk material, E	1.93 x 10^{11} Pa
Thickness of Disks, h	0.16 m
Shaft Section's Area Moment of Inertia, I_s	3.472 x 10^{-4} m4
Disk-1 Area Moment of Inertia, I_1	0.0642 m^4
Disk2 Area Moment of Inertia, I_2	0.0642 m^4
Shaft's Polar Moment of Area, J_{ps}	6.944 x 10^{-4} m^4
Disk-1's Polar Moment of Area, J_{p1}	0.129 m^4
Disk-1's Polar Moment of Area, J_{p2}	0.129 m^4
Mass of Disk 1, M_1	1035.2 kg
Mass of Disk 2, M_2	1035.2 kg

5.1.1 Critical Speeds (Natural Frequency) and the Campbell Diagram

Using Equations (4.23), (4.24) and (4.25), Equivalent mass (M_i, Equivalent Damping Coefficient (C_i), and Stiffness (K_i) for the first mode of transverse vibration are found to be

Table 5.2: *Equivalent Parameters for the first mode*

Equivalent Parameters	**First Mode**
Mass (M_i	1758.48 kg
Damping Coefficient (C_i	3880.74Ω N. s/m
Stiffness (K_i	342530255 – 1758.47Ω^2 N.m

The Equations (4.34) and (4.35) can be used to find the natural frequencies corresponding to the backward whirl and forward. These values are tabulated in **Table 5.3.**

Table 5.3: *Natural Frequencies corresponding to BW and FW*

Spin Speed (Ω) rad/s	**BW frequency** (λ_1) hertz	**FW frequency** (λ_2) hertz
0	70.24	70.24
100	53.20	88.11
200	38.13	106.41
300	28.35	124.927
400	29.68	143.59
500	41.05	162.35

This can be presented in the form of Campbell diagram as shown in **Figure 5.1**.

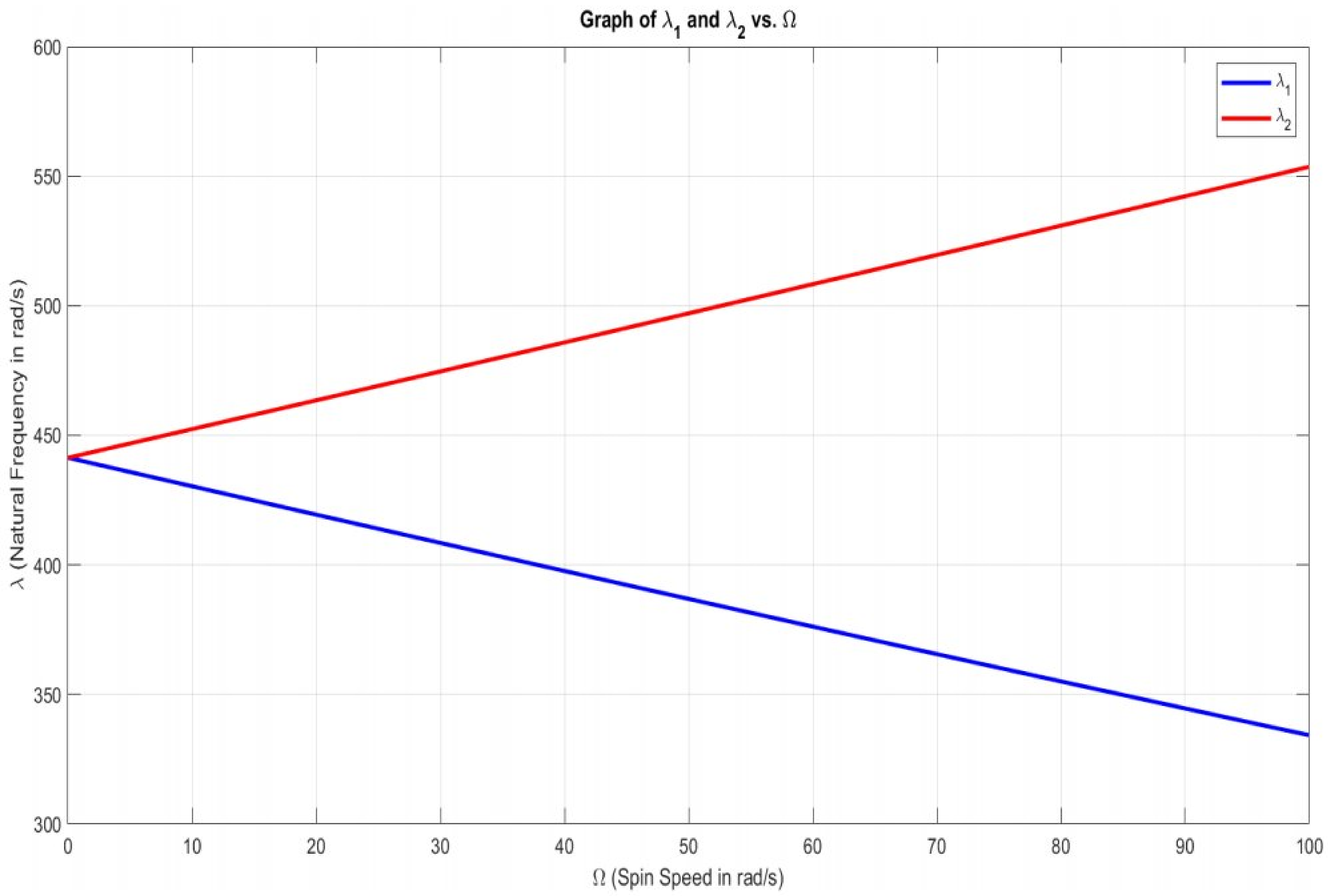

Figure 5.1: *Campbell diagram for the Euler-Bernoulli Beam Model's First Mode*

The mathematical model based upon Euler-Bernoulli beam theory generated this graph. It aims to visualize the natural frequencies of the rotor system as functions of the rotational speed.

The graph typically plots natural frequencies (vertical axis) against the rotational speed (horizontal axis). Each line represents a mode of vibration, with intersections indicating critical speeds where resonance can occur.

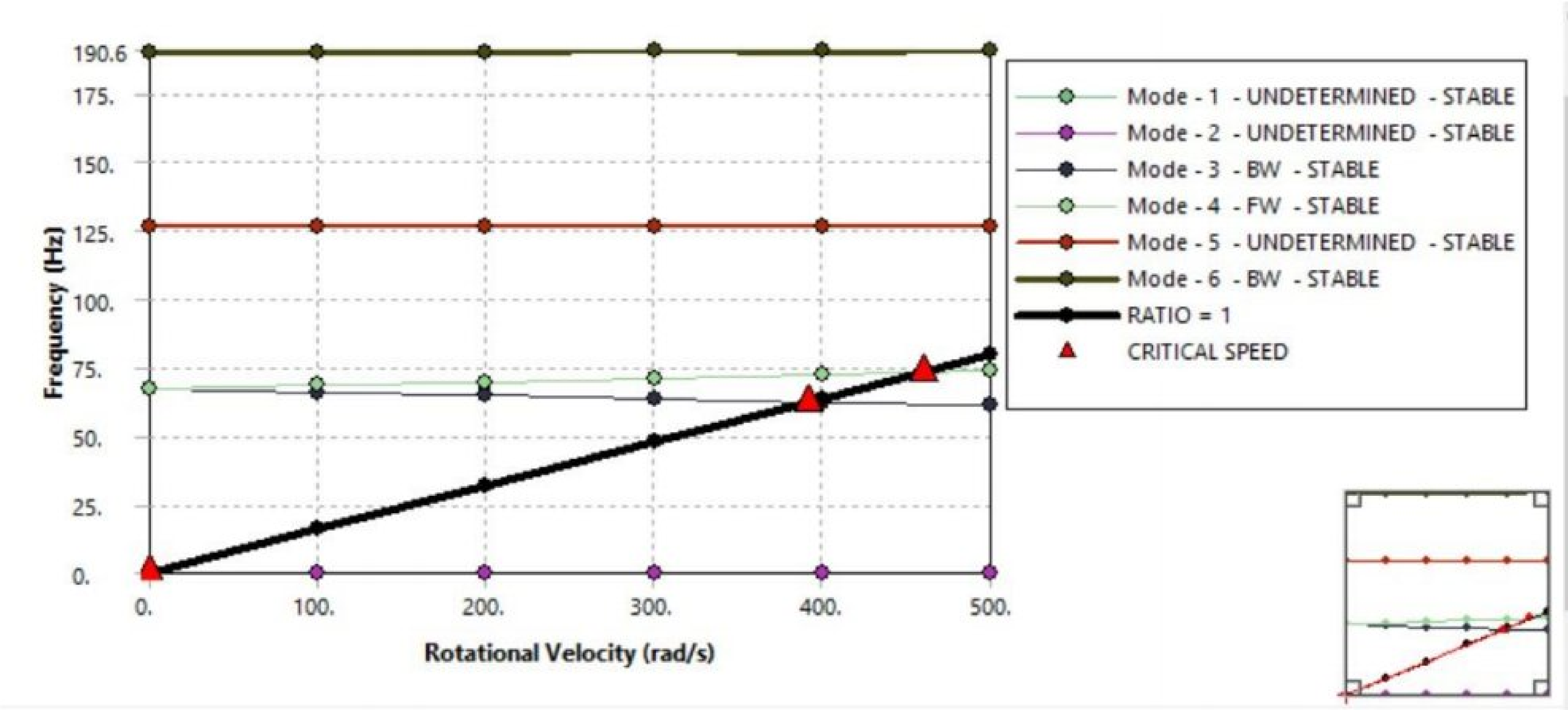

Figure 5.2: *Campbell diagram developed by using ANSYS*

The natural frequencies associated with zero spin speed are equivalent to the first mode's natural frequency of a simply supported beam. The critical speed for forward whirl increases and the critical speed for backward whirl lowers for each mode as the spin speed increases. At lower speeds, the bending stiffness surpasses the centrifugal effect's stiffness. In the case of backward whirl, centrifugal stiffening counteracts the elastic restoring force, leading to a decline in critical speed with increasing spin speed (refer to **Figure 5.1**). On the other hand, during forward whirl, the critical speed increased with greater spin speeds as a result of the centrifugal stiffening aligning with elastic restoring force. (see **Figure 5.1**).

The results obtained from the modal analysis are illustrated in Campbell's diagram in Figure 5.2 above. For the first mode of transverse vibration, mode stability was found to be stable with a critical velocity of 459.83 rad/s. The natural frequency corresponding to the first mode of transverse vibration of the system obtained from the modal analysis were tabulated in table 5.4.

Table 5.4: *Natural frequencies correspond to the first mode of transverse vibration obtained computationally*

Spin Speed (Ω) rad/s	**Forward whirl natural frequency (λ) hertz**
0	67.155
100	72.437
200	94.736
300	110.051
400	125.380
500	140.723

The mathematical model and simulation successfully validated the natural frequency of the first mode of transverse vibration, demonstrating their consistency and accuracy.

CHAPTER SIX: CONCLUSIONS AND RECOMMENDATIONS

6.1 Conclusions

In this study, a multi-rotor system's modal behavior is examined using Euler-Bernoulli Beam model. In this model for bending vibrations in transverse motion, the linked set of differential equations is recognized as the governing equations.

Through a comprehensive free vibration analysis, critical speeds of the system for an operational speed of omega = 500 rad/s are determined for the first transverse mode within the Euler-Bernoulli beam model. The critical speeds are found to be 162.35 Hz for a forward whirl and 41.05 Hz for a backward whirl. Modal analysis using ANSYS reveals critical speeds of 140 Hz for a forward whirl and 55.21 Hz.

Subsequent steps following the research could involve a sensitivity analysis to gain insights into how the system reacts to changes in parameters, conduction experimental validation to verify the analytical and numerical results, implementing structural improvements guided by the critical speed findings, sharing research outcomes through publication and knowledge dissemination, utilizing the research findings for educational purposes, and investigating opportunities for interdisciplinary applications to incorporate the research into interconnected fields.

6.2 Recommendations

In conclusion, this thesis has successfully employed analytical modelling and ANSYS simulations to look at the modal properties of a system of multi-disk rotor with an uneven mass. The findings provide valuable insights into the critical speeds for forward and backward whirls under free vibration. However, further research can extend this knowledge and address areas identified in this study.

One key recommendation is to delve into the non-linear behaviour of these systems, particularly when multiple unbalanced masses or high speeds are involved. Developing analytical and numerical tools to capture this non-linearity would provide a more comprehensive understanding of real-world rotor system dynamics. Additionally, exploring active and passive control techniques presents an exciting opportunity. This research could contribute significantly to improved rotor system performance by investigating methods to dampen vibrations and enhance stability.

Furthermore, a systematic study is recommended on how parameters like the number of disks and unbalanced mass distribution affect the dynamic response. This would provide valuable knowledge for optimising rotor system design. Future research should incorporate real-world experimental validation alongside the analytical and simulation approaches to strengthen the developed models' confidence. Finally, exploring interdisciplinary applications, such as control engineering or material science, could lead to groundbreaking rotor system analysis and design advancements. By pursuing these recommendations, this research can pave the way for a deeper understanding and improved performance of multi-disk rotor systems.

REFERENCES

1. Chen, X., Zhai, J., Zhang, H., & Han, Q. (2020). Simulation study on unbalance vibration characteristics of dual-rotor system. *SN Applied Sciences*, *2*(8). https://doi.org/10.1007/S42452-020-03237-5
2. Cherif, Z. H., & Kandouci, C. (2020). Dynamic Characteristics of Multi-Disk Shaft System using the Vectors of Solution Coefficients. *Journal of Mechanical Engineering*, *17*(3), 95–115. https://doi.org/10.24191/JMECHE.V17I3.15315
3. Childs, D. (1993). *Turbomachinery Rotordynamics: Phenomena, Modeling, and Analysis*. 496. https://www.wiley.com/en-ie/Turbomachinery+Rotordynamics%3A+Phenomena%2C+Modeling%2C+and+Analysis-p-9780471538400
4. Kandouci, C., Adjal, Y., Cherif, Z. H., & Tayeb, R. (2023). Whirling analysis of unbalanced rotor using the vectors of solution coefficients. *Https://Doi.Org/10.1177/10775463231198897*. https://doi.org/10.1177/10775463231198897
5. Khadem, S. E., Shahgholi, M., & Hosseini, S. A. A. (2010). Primary resonances of a nonlinear in-extensional rotating shaft. *Mechanism and Machine Theory*, *45*(8), 1067–1081. https://doi.org/10.1016/j.mechmachtheory.2010.03.012
6. Khadem, S. E., Shahgholi, M., & Hosseini, S. A. A. (2011). Two-mode combination resonances of an in-extensional rotating shaft with large amplitude. *Nonlinear Dynamics*, *65*(3), 217–233. https://doi.org/10.1007/s11071-010-9884-2
7. Khanlo, H. M., Ghayour, M., & Ziaei-Rad, S. (2011). Chaotic vibration analysis of rotating, flexible, continuous shaft-disk system with a rub-impact between the disk and the stator. *Communications in Nonlinear Science and Numerical Simulation*, *16*(1), 566–582. https://doi.org/10.1016/j.cnsns.2010.04.011
8. Kushwaha, N., & Patel, V. N. (2023). Nonlinear dynamic analysis of two-disk rotor system containing an unbalance influenced transverse crack. *Nonlinear Dynamics*, *111*(2), 1109–1137.

https://doi.org/10.1007/S11071-022-07893-7

9. Ling, F. F. (n.d.). *Dynamics of Rotating Systems (Mechanical Engineering Series).*

10. Luintel, M. C. (n.d.-a). *Dynamic Modelling and Response of a Pelton Turbine Unit Dynamic Response of Overhung Pelton Turbine Unit for Forced Vibration View project Dynamic Analysis of Pelton Turbine and Assembly View project*. https://doi.org/10.13140/RG.2.2.34011.82728

11. Luintel, M. C. (n.d.-b). *Dynamic Modelling and Response of a Pelton Turbine Unit Dynamic Response of Overhung Pelton Turbine Unit for Forced Vibration View project Dynamic Analysis of Pelton Turbine and Assembly View project*. https://doi.org/10.13140/RG.2.2.34011.82728

12. *(PDF) Delevitation modelling of an active magnetic bearing supported rotor*. (n.d.). Retrieved 20 June 2024, from https://www.researchgate.net/publication/305422666_Delevitation_modelling_of_an_active_magnetic_bearing_supported_rotor

13. *(PDF) In-Plane Dynamics of High-Speed Rotating Rings on Elastic Foundation*. (n.d.). Retrieved 20 June 2024, from https://www.researchgate.net/publication/338339161_In-Plane_Dynamics_of_High-Speed_Rotating_Rings_on_Elastic_Foundation

14. Shahgholi, M., & Esmaeilzadeh Khadem, S. (2012). Resonance analysis of gyroscopic nonlinear spinning shafts with parametric excitations and speed fluctuations. *International Journal of Mechanical Sciences*, *64*(1), 94–109. https://doi.org/10.1016/J.IJMECSCI.2012.07.010

15. Shahgholi, M., & Khadem, S. E. (2012). Primary and parametric resonances of asymmetrical rotating shafts with stretching nonlinearity. *Mechanism and Machine Theory*, *51*, 131–144. https://doi.org/10.1016/J.MECHMACHTHEORY.2011.12.012

16. Miranda, W. M., & Faria, M. T. (2014). Finite Element Method Applied to the Eigen value Analysis of Flexible Rotors Supported by Journal Bearings. Engineering, 127-137

17. Dr. R. Tiwari; 2014; Torsional Vibrations of Rotors: The Direct and

Transfer Matrix Methods: Three-Disc Rotor System; Nptel & IIT Guwahati.

18. O. Gundogdu,2013; Modelling and Analysis of a Jeffcott Rotor As a Continuous Cantilever Beam and an Unbalanced Disk System; Atatruk University, Faculty of Engineering.
19. Reddy, M., & Srinivas, J. (2016). Vibration Analysis of a Support Excited Rotor System with Hydrodynamic Journal Bearing. Procedia Engineering, 825-832.
20. Alahamadi, A., & Diken, H. (2018). Modelling and Vibration Analyses of a rotor having multiple disks supported by a continuous shaft for the first three modes. International Journal of Modern Research in Engineering and Technology (IJMRET), Volume 3 Issue 7.